

Signatures of pressure-induced superconductivity in insulating $\text{Bi}_{1.98}\text{Sr}_{2.06}\text{Y}_{0.68}\text{CaCu}_2\text{O}_{8+\delta}$ T. Cuk,¹ D. A. Zocco,² H. Eisaki,³ V. Struzhkin,⁴ F. M. Grosche,⁵ M. B. Maple,² and Z.-X. Shen⁶¹*Materials Science Division, Lawrence Berkeley National Laboratory, University of California-Berkeley, Berkeley, California 94720, USA*²*Department of Physics, University of California-San Diego, La Jolla, California 92093, USA*³*Nanoelectronics Research Institute, National Institute of Advanced Industrial Science and Technology, 1-1-1 Central 2, Umezono, Tsukuba, Ibaraki 305-8568, Japan*⁴*Geophysical Laboratory, Carnegie Institution of Washington, 5241 Broad Branch Road NW, Washington, DC 20015, USA*⁵*Department of Physics, Royal Holloway, University of London, Egham, Surrey TW20 0EX, United Kingdom*⁶*Stanford Institute for Materials and Energy Sciences, SLAC National Accelerator Laboratory, Menlo Park, California 94025, USA and Departments of Physics and Applied Physics, Stanford University, Stanford, California 94305, USA*

(Received 19 February 2010; revised manuscript received 20 April 2010; published 12 May 2010)

We have performed several high-pressure electrical resistance experiments on $\text{Bi}_{1.98}\text{Sr}_{2.06}\text{Y}_{0.68}\text{Cu}_2\text{O}_{8+\delta}$ (Bi2212), an insulating parent compound of the high- T_c Bi2212 family of copper oxide superconductors. We find a resistive anomaly, a downturn at low temperature, that onsets with applied pressure in the 20–40 kbar range. Through both resistance and magnetoresistance measurements, we identify this anomaly as a signature of induced superconductivity. Resistance to higher pressures decreases T_c , giving a maximum of ~ 10 K. The higher pressure measurements exhibit a strong sensitivity to the hydrostaticity of the pressure environment. We make comparisons to the pressure-induced superconductivity now ubiquitous in the iron arsenides.

DOI: [10.1103/PhysRevB.81.184509](https://doi.org/10.1103/PhysRevB.81.184509)

PACS number(s): 74.25.Dw, 74.72.-h, 74.62.Fj, 74.25.F-

I. INTRODUCTION

The recently discovered class of iron arsenide superconductors have been compared to the high- T_c copper oxide superconductors based on the proximity of the superconducting dome to an antiferromagnetic phase in the doping phase diagram and the planarlike sheets in which the superconductivity lies.¹ In both classes of high- T_c families, the phase diagram exhibits a large range of structural, charge, and magnetic instabilities that manifest themselves more strongly in one specific compound or at a particular doping than another. Given the complexities of understanding how physical parameters are changed by chemical doping, pressure has been sought as a laboratory controlled variable to tune a single parent compound across the phase diagram. In the iron arsenide compounds, pressure-induced superconductivity has already been found in CaFe_2As_2 ,² BaFe_2As_2 ,³ SrFe_2As_2 ,³ and LaFeAsO .⁴ The pressure-induced superconductivity appears as the tetragonal to orthorhombic structural transition temperature is lowered and the associated spin- and charge-density-wave transitions weaken.⁵ In the cuprates, by contrast, pressure-induced superconductivity of the parent, or weakly doped, compounds has not been found.

Similar to the iron arsenide compounds, there are several mechanisms by which pressure could induce metallicity in the cuprate parent insulators. By decreasing the Cu-O bond distance, the $\text{Cu}_d\text{-O}_p$ hybridization increases and the Cu_d band further delocalizes. Second, the relatively higher c -axis compressibility facilitates electron or hole doping by bringing the chemically substituted charge reservoir layers closer to the Cu-O plane.⁹ Preferred compression along the layered c axis also increases the interlayer tunneling matrix element (t_\perp).^{6,7} Finally, contraction of the lattice changes electron-electron and electron-phonon interactions by varying both electron screening and crystal fields.⁸

Past pressure experiments on superconducting $\text{Bi}_2\text{Sr}_2\text{CaCu}_2\text{O}_8$ (Bi2212) have indeed shown significant increase in T_c on the underdoped side of the superconducting

dome,⁸ attributed to a pressure-induced doping as inferred from Hall effect measurements.⁹ However, pressure leads to higher T_c 's for even overdoped Bi2212 compounds, which suggests that the strength of the Cooper-pair coupling also changes.⁸ Similar results are found for $\text{YBa}_2\text{Cu}_3\text{O}_7$.^{9–12} The sensitivity of the c -axis resistivity in $\text{Bi}_2\text{Sr}_2(\text{Ca},\text{Y})\text{Cu}_2\text{O}_8$ and $\text{YBa}_2\text{Cu}_3\text{O}_7$ to uniaxial pressure has been attributed to increased interlayer tunneling t_\perp .^{6,7}

Recently, pressure has tuned insulating Bi2212 across an electronic transition seen by Raman spectroscopy at high (200 kbar) pressures.¹³ The electronic transition coincides with a change in the behavior of the magnons, the phonons, and the c/a lattice constant ratio. So far, however, pressure-induced superconductivity has not been reported in a parent cuprate compound. In this work, we study the effect of pressure on insulating $\text{Bi}_2\text{Sr}_2\text{CaCu}_2\text{O}_8$ in resistance measurements using two different Bridgman-anvil cell setups and a diamond-anvil cell (DAC). We identify a broad downturn at $\sim 8\text{--}10$ K occurring at ~ 30 kbar, as a signature of induced superconductivity. In all three experiments, the resistive downturn indicative of superconductivity is observed to have an onset in the 20–40 kbar range. However, the high-pressure range (above 40 kbar) differs due to the variations in hydrostaticity. A higher c -axis stress is correlated with a more extended range of induced superconductivity and an enhanced metallic behavior. Finally, we compare these results to the pressure-induced superconductivity seen in the iron arsenides.

II. EXPERIMENTAL DETAILS

Single crystals of $\text{Bi}_{1.98}\text{Sr}_{2.06}\text{Y}_{0.68}\text{Cu}_2\text{O}_{8+\delta}$ (Bi2212) were grown by the floating-zone method and have a doping dependence of T_c described by Maeda¹⁴ and Terasaki.¹⁵ Given the sensitivity of these samples to the hydrostaticity of the pressure environment, we report results using three different pressure configurations. In all three of the anvil cells, the a, b

plane of the sample is placed on the flat surface of the anvil, such that the c axis lies along the central axis of the anvil, and the contacts are placed on top of one of the a , b planes to measure a combination of the a , b resistance. In the first, a sample of $1 \times 0.25 \times 0.025$ mm³ was loaded in a beryllium-copper Bridgman-anvil clamped cell (BAC1) using solid stearite as the quasihydrostatic pressure transmitting medium. The pressure was determined from the superconducting transition of a strip of Pb foil placed adjacent to the sample. Electrical resistivity was measured with a standard four-point technique and a LR-700 ac resistance bridge using four flattened 50 μ m platinum wires for each the sample and the Pb. Silver pads of DuPont 7095 silver paste were made in order to achieve better electrical contacts. This was the most hydrostatic configuration achieved. In the second configuration, a sample of $0.8 \times 0.2 \times 0.02$ mm³ (length width height (LWH)) was also loaded into a Bridgman anvil cell (BAC2) next to a Pb manometer. Calcium sulfate powder served as a transparent pressure medium instead. The electrical contacts for the sample and Pb manometer were obtained as in the BAC1 experiment. The magnetoresistance measurements reported for BAC2 were performed with a Quantum Design physical property measurement system (PPMS) instrument. In BAC2, we report results from the two-point measurements alone due to complications with a nonhomogeneous pressure environment. The width of the Pb transition is a measure of pressure inhomogeneity along the Pb manometer: ± 2 kbar in BAC1 and ± 5 kbar in BAC2. In the third configuration, the samples were loaded into a DAC with argon gas as the pressure transmitting medium. The $\sim 0.03 \times 0.03 \times 0.005$ mm³ Bi2212 samples were glued onto one of the diamond anvils and Pt leads were, with a focus ion beam, milled directly onto the top and side surfaces of the sample in a four-point configuration and then extended along the diamond to meet the gasket leads. The gasket was made of a boron nitride/epoxy mixture and ruby chips served as pressure markers. In the DAC, measurements of ruby chips placed at opposite ends of the sample estimate the degree of nonhydrostaticity/ c -axis uniaxial pressure to be 20 kbar at the highest pressures. In all experimental configurations, pressure was increased at room temperature; pressure values were recorded at low temperature since the pressure remains almost constant below 100 K.

From BAC1 to BAC2 to the DAC experiments, the degree of nonhydrostaticity/ c -axis uniaxial stress, increases. The contact configuration and pressure medium determine the level of hydrostaticity.¹⁶ In BAC1, stearite and thin Pt wires are used as opposed to the less hydrostatic calcium sulfate and thicker Pt wires in BAC2. In the DAC experiments, while argon can be more hydrostatic than a solid powder medium in the lower pressure ranges, it solidifies at the measured temperatures and pressures (below 80 K at ambient pressure).^{17,18} Moreover, in the DAC experiments, the sample is glued to the diamond surface on which the Pt leads are milled; only one side of the sample sees the quasihydrostatic medium. While the DAC configuration has the least hydrostatic environment, it makes pressures in the 100's kbar range available. The pressure gradients measured via ruby fluorescence measurements in the DAC (20 kbar), and the width of the Pb superconducting transition in BAC1 (2 kbar)

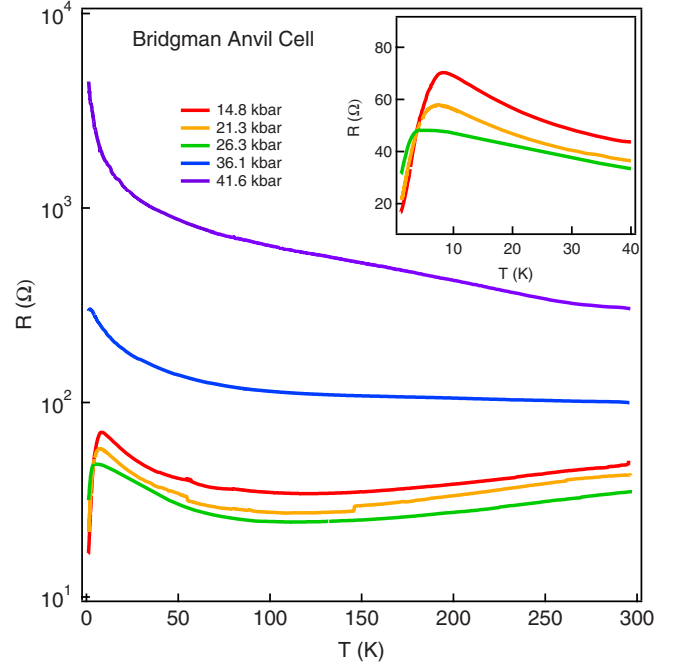


FIG. 1. (Color online) Resistance vs temperature shown on a log scale for different pressures for $\text{Bi}_{1.98}\text{Sr}_{2.06}\text{Y}_{0.68}\text{Cu}_2\text{O}_{8+\delta}$ loaded in BAC1. Inset: low temperature resistance drop on a linear scale for selected pressures.

and BAC2 (5 kbar) corroborate these assessments.

III. RESULTS

Figure 1 shows the temperature-dependent resistance of the sample loaded in BAC1 at different pressures. By 15 kbar, the insulating characteristic of the unpressurized sample has become a downturn below 8 K of 50 Ω . With increasing pressure, the T_c of the downturn lowers and the magnitude decreases (see inset). By 36 kbar, the T_c decreases to 2 K, and by 40 kbar, the sample is completely insulating to 1.8 K. Above 8 K, the insulating rise initially decreases with pressure, indicating a more metallic sample, but increases significantly beyond ~ 30 kbar along with the overall resistance.

Figure 2 shows the temperature-dependent resistance and magnetoresistance of the sample loaded in BAC2 at different pressures. In Fig. 2(a), the resistance decreases by four orders of magnitude between 8 and 25 kbar. Though not as pronounced as in BAC1, the insulating characteristic becomes a downturn at low temperatures—most pronounced at 25 kbar [Fig. 2(b)] but also apparent at 8 kbar [see inset to Fig. 2(a)]. In these experiments, we applied a magnetic field and found that the resistive anomaly was almost totally suppressed with an applied field of 9 T [Fig. 2(b)]. We use this positive magnetoresistance (increasing resistance with applied magnetic field) as another measure of the induced superconductivity. Since the magnon peak is not suppressed in this pressure range, as seen earlier by pressure-dependent Raman studies,¹³ the positive magnetoresistance cannot be attributed to a suppression of short-range antiferromagnetic

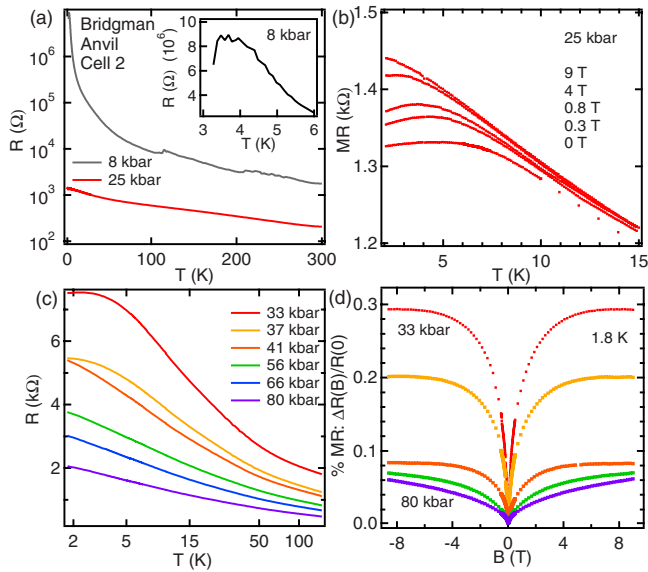


FIG. 2. (Color online) $\text{Bi}_{1.98}\text{Sr}_{2.06}\text{Y}_{0.68}\text{Cu}_2\text{O}_{8+\delta}$ loaded in BAC2. (a) Resistance vs temperature for two selected pressures in the lower pressure range. (b) Magnetoresistance vs temperature for several different magnetic fields at 25 kbar, where the low-temperature resistive anomaly was observed. (c) Resistance vs temperature for the higher pressure range plotted on a $\ln T$ scale. (d) Magnetic field sweeps for the curves shown in (c).

order.¹⁹ We show sweeps in magnetic field for several pressures at 1.8 K in Fig. 2(d). The largest magnetoresistance is observed in the range of 30 kbar and decreases significantly beyond 40 kbar. Like in BAC1, then, the induced signatures of superconductivity disappear with continued increase in pressure. The high magnetoresistance occurs for those pressures that show either a flattening or a downturn of the resistance at low temperatures [Fig. 2(c)]. Further increase in pressure continues to make the sample more metallic [Fig. 2(c)] and in contrast to BAC1, continues to become increasingly more metallic up to 80 kbar. Beyond ~ 50 kbar, we find a $\ln T$ (K) dependence over two decades in temperature. We see this same trend in the BAC1 measurements shown in Fig. 1, in the pressure range of 14–16 kbar, where the superconductivity is most pronounced. This same characteristic is prominent in $\text{Bi}2201$ samples near the dome²⁰ and when superconductivity is suppressed by the application of a magnetic field in $\text{Bi}2201$.²¹

In both BAC1 and BAC2, the strongest signatures of superconductivity occur below 40 kbar. In Fig. 3, we graph T_c vs pressure for both cells. T_c is determined by the temperature at which the high-temperature slope diverges from the low-temperature behavior. Even at 8 kbar we find a downturn at 4 K, which suggests that as with the pressure-induced superconductivity in the iron pnictides, T_c traces a dome with pressure.^{16,22–24} In the region beyond 40 kbar, the results in BAC1 and BAC2 differ substantially: in BAC1, we observe the return of an insulating state, whereas in BAC2, we find resistance curves similar to those of doped samples near the dome.

Finally, in Fig. 4, we show the results from the DAC experiments. In the DAC we were unable to reach pressures

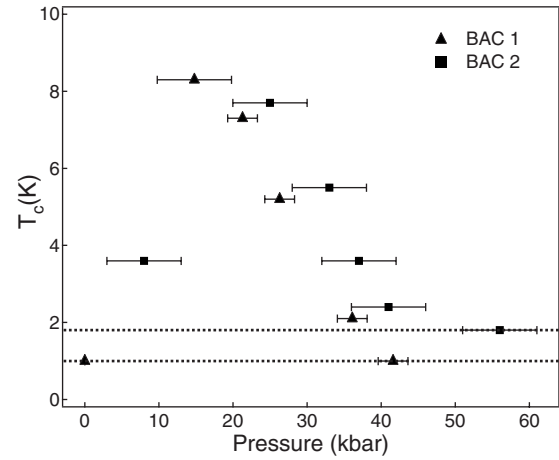


FIG. 3. T_c vs pressure for $\text{Bi}_{1.98}\text{Sr}_{2.06}\text{Y}_{0.68}\text{Cu}_2\text{O}_{8+\delta}$ loaded in BAC1 and BAC2. The lowest measured temperatures for BAC1 and BAC2 are indicated by the dotted lines. Error bars on the pressure points are taken from the width of the Pb superconducting transition and indicate the uniaxial stress along the c axis.

lower than 70 kbar without releasing the gas medium. From 70 to 140 kbar, we find a downturn again indicating induced superconductivity. With pressure, the downturn moves from 10 K to lower temperatures, reaching 5 K by 170 kbar. Similar to the BAC results, beyond a certain pressure, the superconducting signature diminishes. However, in strong contrast to the BAC results, the superconducting signature extends to 170 kbar where in the BAC it ends at 50 kbar. In further contrast to the BAC results, above 10 K, the sample is purely metallic up to 300 K (see inset) and through the highest measured pressures. We attribute this metallic behavior and extended superconductivity to the higher c -axis stress in the DAC: greater than in the BAC due to both the solid argon pressure medium at low temperatures and the milled Pt wires (see experimental section). As discussed in Sec. I, a higher c -axis stress can lead to enhanced metallic behavior by

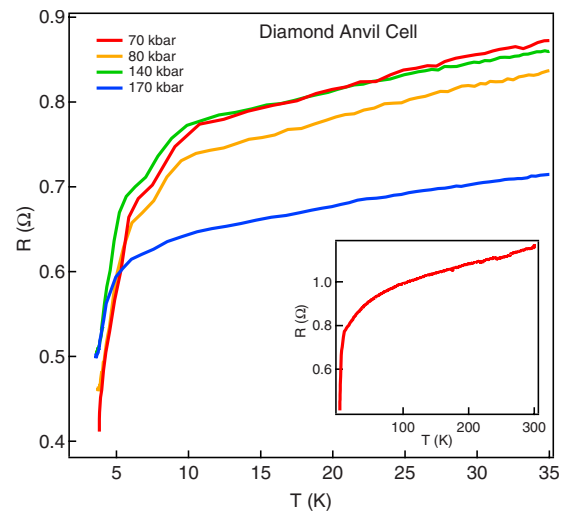


FIG. 4. (Color online) Resistance vs temperature for $\text{Bi}_{1.98}\text{Sr}_{2.06}\text{Y}_{0.68}\text{Cu}_2\text{O}_{8+\delta}$ loaded in the DAC in the low-temperature range. Inset: resistance curve at 70 kbar for the entire temperature range.

bringing the charge reservoir layers closer to the Cu-O plane, enhancing interlayer tunneling, and changing electron-electron and electron-phonon interactions through the crystal field along the c axis.

IV. DISCUSSION AND SUMMARY

We find a signature of superconductivity occurring in insulating Bi2212 between 20–40 kbar in the BAC experiments, extending to 170 kbar in the DAC. If one considers the parent copper oxide insulators as Mott insulators, such a low-pressure onset of superconductivity is not expected. A classic Mott insulator such as MnO only reaches metallization at 100 GPa.²⁵ Therefore, these superconducting signatures are not likely the result of a Mott gap collapsing through simple hybridization of in-plane Cu-O orbitals.

Even though superconductivity seems to onset at much lower pressures, T_c reaches at most 10 K. In the iron arsenide compounds, the T_c under pressure has been shown to reach 30 K,^{3,4,26} approximately the T_c of the optimally doped parent compound at ambient pressure. In our experiments with Bi2212, T_c under pressure only reaches a fraction of the optimally doped value of ~ 100 K. On the other hand, it is somewhat surprising that in both classes of high- T_c superconductors, signatures of superconductivity can be seen in the form of broad resistance curves^{4,26} by the same pressure of ~ 30 kbar. One possible outlook is that the superconductivity taking place in the copper oxides with doping are of two forms: one that can be traced to lower pressures, and bearing similarity to the pressure-induced superconductivity of the iron arsenides, and another higher T_c superconductivity that has only been accessed by doping so far. In the recent Raman spectroscopy experiments carried out in Bi2212 samples under pressure, it was possible to identify an electronic transition at 200 kbar with an anomaly occurring in the lattice constant ratio c/a .¹³ It is worth mentioning that a similar, though more dramatic, decrease occurs in c/a when CaFe_2As_2 enters the collapsed tetragonal state²⁷ at much lower pressures.

The absence of full resistive transitions suggests that superconductivity is induced in a small volume fraction of the sample by a favorable combination of local sample composition and local strain. The dopant charge is not fully donated to the Cu-O plane in these compounds and, therefore, hole count depends on the distance of the Cu-O plane to the dopants. Therefore sample inhomogeneity (known to be prevalent in $\text{Bi}_{1.98}\text{Sr}_{2.06}\text{Y}_{0.68}\text{Cu}_2\text{O}_{8+\delta}$) and inhomogeneity in the strain will strongly influence the percolation pathway measured by resistivity. Phase separation could play an essential role in determining the properties of the superconducting state, with a fraction of the sample becoming superconducting under pressure, and the remaining fraction remaining in the antiferromagnetic state.²⁸ Yet, calculations based on the local-density approximation (taking into account the distance of the Cu-O plane to the charge-transfer layers) suggest that even a nominally homogeneous parent insulator can reach the dome with modest pressures. Estimates of hole count give 0.008 holes/Cu/GPa for both underdoped and optimally

doped samples,¹⁰ which would suggest that a slightly doped parent insulator could reach the dome by 5 GPa (0.05 hole/Cu) and optimal doping (0.2 hole/Cu) by 20 GPa. Further work will be required to elucidate the precise conditions under which the transitions reported here will spread to the bulk, but the key finding—that signatures of superconductivity can be induced in Bi2212 by externally applied stress—is robust.

It is unlikely that a more hydrostatic environment will induce a higher T_c in the cuprates. For the largest downturn and highest T_c measured in BAC1, the pressure gradients at 14 kbar approached ± 5 kbar (see Fig. 3) and only decreased at higher pressures where the superconductivity weakened. Moreover, we attempted the same experiments in hydrostatic piston cylinder cells and little change is observed up to 24 kbar. Such an observation is not unexpected: clear differences are observed for CePd_2Si_2 in which anvil cells report strong enhancement of T_c and a doubled pressure range in which the superconductivity occurs compared to piston-cylinder cells.²⁹ Furthermore, comparisons with the iron arsenides also suggest that a more hydrostatic environment may not enhance T_c . CaFe_2As_2 does not become superconducting under ideal hydrostatic pressure conditions¹⁶ and internal strain coming from c -axis-orientated planar defects in SrFe_2As_2 promotes superconductivity.³⁰

Instead, one option for future experiments is to apply a purely c -axis stress to see if a more robust superconductivity can be induced. In particular, since the c axis has the highest compressibility and also has the highest applied stress in the current experimental setup, one can think of the distance between the Cu-O planes and the intervening charge reservoir layers as tuning four separate microscopic quantities: charge transfer and disorder (by bringing the dopants closer to the plane), interlayer tunneling (decreasing t_\perp), and increasing the crystal field across the Cu-O plane. Some of these effects, such as charge transfer and disorder or the crystal field and charge transfer, will compete to determine the induced superconductivity. It is an open question whether or not these competing effects can be controlled with a parameter other than doping to achieve the optimal T_c of the copper oxide family.

ACKNOWLEDGMENTS

We would like to acknowledge helpful discussions with A. Kapitulnik, E. Gregoryanz, A. Mackenzie, and M. Núñez Regueiro. T. Cuk would like to thank the Royal Holloway, University of London for the use of facilities and access to pressure cells. T. Cuk would also like to thank the Carnegie Institution of Washington for the use of facilities, and partial support of this work. The Stanford work was supported by DOE Office of Science, Division of Materials Science, with Contract No. DE-FG03-01ER45929-A001 and NSF under Grant No. DMR-0304981. Research at University of California, San Diego was supported by the National Nuclear Security Administration under the Stewardship Science Academic Alliance Program through the U.S. Department of Energy under Grant No. DEFG52-06NA26205.

- ¹M. Rotter, M. Tegel, and D. Johrendt, *Phys. Rev. Lett.* **101**, 107006 (2008).
- ²M. S. Torikachvili, S. L. Bud'ko, N. Ni, and P. C. Canfield, *Phys. Rev. Lett.* **101**, 057006 (2008).
- ³P. L. Alireza, Y. T. Chris Ko, J. Gillett, C. M. Petrone, J. M. Cole, G. G. Lonzarich, and S. E. Sebastian, *J. Phys.: Condens. Matter* **21**, 012208 (2009).
- ⁴H. Okada, K. Igawa, H. Takahashi, Y. Kamihara, M. Hirano, H. Hosono, K. Matsubayashi, and Y. Uwatoko, *J. Phys. Soc. Jpn.* **77**, 113712 (2008).
- ⁵M. S. Torikachvili, S. L. Bud'ko, N. Ni, and P. C. Canfield, *Phys. Rev. B* **78**, 104527 (2008).
- ⁶L. Forró, V. Ilakovac, and B. Keszei, *Phys. Rev. B* **41**, 9551 (1990).
- ⁷M. F. Crommie, A. Y. Liu, A. Zettl, M. L. Cohen, P. Parilla, M. F. Hundley, W. N. Creager, S. Hoen, and M. S. Sherwin, *Phys. Rev. B* **39**, 4231 (1989).
- ⁸X.-J. Chen, V. V. Struzhkin, R. J. Hemley, H. K. Mao, and C. Kendziora, *Phys. Rev. B* **70**, 214502 (2004).
- ⁹C. Murayama, Y. Iye, T. Enomoto, N. Mōri, Y. Yamada, T. Matsumoto, Y. Kubo, Y. Shimakawa, and T. Manako, *Physica C* **183**, 277 (1991).
- ¹⁰J. D. Jorgensen, S. Pei, P. Lightfoot, D. G. Hinks, B. W. Veal, B. Dabrowski, A. P. Paulikas, R. Kleb, and I. D. Brown, *Physica C* **171**, 93 (1990).
- ¹¹S. Klotz, W. Reith, and J. S. Schilling, *Physica C* **172**, 423 (1991).
- ¹²S. W. Tozer, J. L. Koston, and E. M. McCarron III, *Phys. Rev. B* **47**, 8089 (1993).
- ¹³T. Cuk, V. Struzhkin, T. P. Devereaux, A. Goncharov, C. Kendziora, H. Eisaki, H. Mao, and Z.-X. Shen, *Phys. Rev. Lett.* **100**, 217003 (2008).
- ¹⁴A. Maeda, M. Hase, I. Tsukada, K. Noda, S. Takebayashi, and K. Uchinokura, *Phys. Rev. B* **41**, 6418 (1990).
- ¹⁵I. Terasaki, T. Takemura, T. Takayanagi, and T. Kitajima, Proceedings of the 12th International Conference on Superconductivity (ISS '99), 1999 (unpublished).
- ¹⁶H. Lee, E. Park, T. Park, V. A. Sidorov, F. Ronning, E. D. Bauer, and J. D. Thompson, *Phys. Rev. B* **80**, 024519 (2009).
- ¹⁷N. Tateiwa and Y. Haga, *Rev. Sci. Instrum.* **80**, 123901 (2009).
- ¹⁸R. J. Angel, M. Bujak, J. Zhao, G. D. Gatta, and S. D. Jacobsen, *J. Appl. Crystallogr.* **40**, 26 (2007).
- ¹⁹Long-range antiferromagnetic order has not yet been established in Bi2212 through neutron scattering.
- ²⁰T. W. Jing, N. P. Ong, T. V. Ramakrishnan, J. M. Tarascon, and K. Reimann, *Phys. Rev. Lett.* **67**, 761 (1991).
- ²¹S. Ono, Y. Ando, T. Murayama, F. F. Balakirev, J. B. Betts, and G. S. Boebinger, *Phys. Rev. Lett.* **85**, 638 (2000).
- ²²H. Takahashi, K. Igawa, K. Arii, Y. Kamihara, M. Hirano, and H. Hosono, *Nature (London)* **453**, 376 (2008).
- ²³D. A. Zocco, J. J. Hamlin, R. E. Baumbach, M. B. Maple, M. A. McGuire, A. S. Sefat, B. C. Sales, R. Jin, D. Mandrus, J. R. Jeffries, S. T. Weir, and Y. K. Vohra, *Physica C* **468**, 2229 (2008).
- ²⁴J. J. Hamlin, R. E. Baumbach, D. A. Zocco, T. A. Sayles, and M. B. Maple, *J. Phys.: Condens. Matter* **20**, 365220 (2008).
- ²⁵C. S. Yoo, B. Maddox, J.-H. P. Klepeis, V. Iota, W. Evans, A. McMahan, M. Y. Hu, P. Chow, M. Somayazulu, D. Häusermann, R. T. Scalettar, and W. E. Pickett, *Phys. Rev. Lett.* **94**, 115502 (2005).
- ²⁶M. Kumar, M. Nicklas, A. Jesche, N. Caroca-Canales, M. Schmitt, M. Hanfland, D. Kasinathan, U. Schwarz, H. Rosner, and C. Geibel, *Phys. Rev. B* **78**, 184516 (2008).
- ²⁷A. I. Goldman, A. Kreyssig, K. Prokeš, D. K. Pratt, D. N. Argyriou, J. W. Lynn, S. Nandi, S. A. J. Kimber, Y. Chen, Y. B. Lee, G. Samolyuk, J. B. Leão, S. J. Poulton, S. L. Bud'ko, N. Ni, P. C. Canfield, B. N. Harmon, and R. J. McQueeney, *Phys. Rev. B* **79**, 024513 (2009).
- ²⁸E. Sigmund, V. Hizhnyakov, R. K. Kremer, and A. Simon, *Z. Phys. B: Condens Matter* **94**, 17 (1994).
- ²⁹A. Demuer, A. T. Holmes, and D. Jaccard, *J. Phys.: Condens. Matter* **14**, L529 (2002).
- ³⁰S. R. Saha, N. P. Butch, K. Kirshenbaum, J. Paglione, and P. Y. Zavalij, *Phys. Rev. Lett.* **103**, 037005 (2009).